https://doi.org/10.5194/os-2021-29
Preprint. Discussion started: 23 April 2021

Ocean Science
Discussions
Open Access
EGU

The inference of internal solitary waves in the northern South China Sea from data acquired by underwater gliders

Wei Ma[1,2], Hongwei Zhang[1], Chenyi Luo[1], Yanhui Wang[1,2], Yang Song[1]

[1] Key Laboratory of Mechanism Theory and Equipment Design of Ministry of Education, School of Mechanical Engineering, Tianjin University, Tianjin, China

[2] Joint Laboratory of Ocean Observation and Exploration, Pilot National Laboratory for Marine Science and Technology, Qingdao, Shandong, China

Correspondence to: Yanhui Wang (email: yanhuiwang@tju.edu.cn)

Abstract. Internal solitary waves (ISWs) are typical large-amplitude nonlinear waves occurring in stratified oceans. The *in situ* observations of ISWs are needed to improve the regimes of nonlinear internal wave theories. There is violent mixing of water mass in the horizontal and vertical directions during the propagation of ISWs, which generally lasts for a short period at a fixed position. However, an underwater glider, with the features of low-speed and sawtooth motion, cannot obtain a complete thermohaline stratification before and after the ISWs arrival. Those thermohaline data collected *in situ* by gliders, which vary synchronously at spatial-temporal scales, raise challenges for identifying the ISWs. Four Petrel-II gliders are deployed in the active region of ISWs in the South China Sea. This paper estimates vertical water velocity from glider flight data and kinematic model, analyzes the sensitivity of parameters in the glider kinematic model, and adopts a standard nonlinear search method to calibrate the parameters insensitive to the vertical velocity. The depth-keeping experiment is performed to verify the effectiveness of the optimized results. The standard deviation of vertical water velocity in the eastern Dongsha Atoll is revealed, and its distribution indirectly reflects that the strength of vertical water activity increases gradually at the same latitude along the east-west direction. Using observations of vertical water velocity fluctuations and isothermal surface vertical displacements, single- and multiple-wave packets can be identified. The availability of this method is tested by comparison with a MODIS image. Such an analysis provides a basis for the application of glider in the observation of ISWs.

Keyword: glider, vertical water mass velocity, single-wave packet, multiple-wave packet

1. Introduction

Internal solitary waves (ISWs) are ubiquitous features in the ocean, and they can propagate over thousands of kilometers from the generation site with unusually strong currents, which may promote the exchange of nutrients and biological production, and threaten the safety of ocean engineering or platforms (Cai et al., 2012; Simmons et al., 2011; Shroyer et al., 2010). To well understand the ISWs, several theories have been proposed (Cai et al., 2014). The *in situ* observation of ISWs contributes to the development of these theories. Major observational methods include 1) remote sensing, which owns the characteristic of large-scale space (Zhao et al., 2004; Jackson, 2007), but with limited capability in sensing the sea surface; 2) moorings, which can obtain high-resolution thermohaline and current structures (Ramp et al., 2004; Alford et al., 2012), whereas conduct observation at a fixed position; 3) research vessels, which can conduct the well-designed and targeted survey in combination with field data (Farmer et al., 2011; Liang

https://doi.org/10.5194/os-2021-29
Preprint. Discussion started: 23 April 2021


Ocean Science
Discussions
Open Access
EGU

et al., 2019), only being time-consuming and costly.

In the previous decades, the autonomous platforms (such as float and glider) played a significant role in the observation of some essential ocean variables. As an important member, gliders have been widely used in the oceanographic measurements (Whitt et al., 2020; Rudnick, 2016; Testor et al., 2019). The glider is driven by a variable buoyancy engine to sink and rise alternately between the surface and a depth of 1000m or more. With the aid of wings, the glider flies along a sawtooth trajectory with the glide speed of 0.25m/s or horizontal distance of ~20km/day. The underwater attitude of glider is adjusted by shifting or rotating the eccentric battery pack (or rudder) under the navigation of electronic compass. Upon surfacing, the glider performs positioning via GPS, communicates with shore-based control center and transmits part of observational data via satellite. The low-power consumption and low-speed cruising enable glider to conduct long endurance missions, which can last several months or up to a year at temporal scales and span several hundreds or even thousands of kilometers on spatial scales.

The observation of internal waves or tides conducted by gliders has been reported in several studies (Rudnick et al., 2013; Boettger et al., 2015; Johnston and Rudnick, 2015; Johnston et al., 2015; Todd, 2017; Hall et al., 2017; Ma et al., 2018; Hall et al., 2019). As a type of nonlinear internal waves, ISWs are very active in the South China Sea (SCS), which exist with amplitudes up to 100m and phase speeds of 0.7~2.9m/s (Cai et al., 2012). The depression wave and elevation wave have different structures and cause contrasting vertical fluctuations of seawater along the direction of wave propagation. The ISWs observed in the SCS could be classified into two categories: a single-wave packet, which contains a single ISW with/without an oscillating tail, and a multiple-wave packet composed of a group of rank-ordered ISWs. According to the *in situ* observation, a conventional solution to identify and classify the waves is to analyze the displacement of isopycnals and isotherms or the fluctuation of currents (Ramp et al., 2004; Ramp et al., 2010; Huang et al., 2016). However, the motion characteristics of glider determine that it cannot achieve the fixed-station observation as moorings to obtain complete thermohaline stratification at different depths before and after ISWs arrival. It is difficulty in identifying and analyzing IWSs using glider observations which mix temporal and spatial scales simultaneously. Therefore, it is questionable to analyze the vertical thermohaline fluctuations to identify ISWs and classify the types of ISWs with the glider.

ISWs in the process of propagation induce strong currents simultaneously, involving horizontal and vertical water velocities. Given the extra costs on the current sensors, the horizontal water velocity measured by gliders is not discussed here. The observation of vertical water velocity by the near-neutral glider has been proven feasible in practice (Merckelbach et al., 2010). The vertical velocity of water mass itself is the difference between the depth-rate measured by pressure transducer from CTD and the glider's velocity through still water, while the latter can be estimated from the kinematic model. With the vertical water velocities derived from the glider, the passage of internal waves can be confirmed, and the intensity of internal waves in the survey area can be mapped (Rudnick et al., 2013; Todd, 2017). Therefore, the vertical water velocity, combined with high-resolution hydrographic data may be a solution to reflect the feature of ISWs, which is presented and verified in this work.

Here, we describe the hydrographic data and glider flight data collected in the northern South China Sea during August 2017. The paper is organized as follows. Section 2 outlines the survey conducted by four gliders. The estimation of vertical water velocities obtained by gliders is introduced in Section 3, and then the approach for identifying and classifying the ISWs is described and then validated by a satellite image (Section 4). Finally, the

https://doi.org/10.5194/os-2021-29
Preprint. Discussion started: 23 April 2021

summary and discussion are presented in Section 5.

2. Glider observation

Four Petrel-II gliders (No. Glider-05/06/08/10), as shown in Fig. 1(a), developed by Tianjin University were prepared for observation of ISWs in the northern South China Sea. According to the statistical analysis of ISWs in the spatial occurrence from synthetic aperture radar (SAR), the ISWs in the northern South China Sea are mainly distributed in the region of Luzon Strait, Dongsha Atoll and eastern Hainan Island (Huang et al., 2008). Most ISWs in the northern South China Sea are generated within Luzon Strait, and propagate westward (Simmons et al., 2011). Those waves present relatively sparse distribution in the region at over 3000m depth than the vicinity of Dongsha Atoll. The Petrel-II glider is designed for applications to 1500m depth and perform best for profiles deeper than 600m. However, in the northwest Dongsha Atoll, the depth of water is less than 500m, and the complicated topography may endanger the glider. The ISWs are concentrated within a longitudinal band from 117°E to 119°E and a latitudinal band from 19°N to 22°N. The gliders were deployed in this region where the water depth is over 1000m and run with approximately parallel trajectories in order to cover this area as wide as possible.

Besides, the occurrence frequencies of ISWs also fluctuate significantly from month to month (Zheng et al., 2007). The ISWs occur more frequently from April to August. According to marine meteorological conditions, 4 Petrel-II gliders conducted ISWs observation cooperatively in August 2017. Those gliders were deployed in the northeast of Dongsha Atoll and then proceeded southwestward and back. The trajectories are shown in Fig. 1(b).

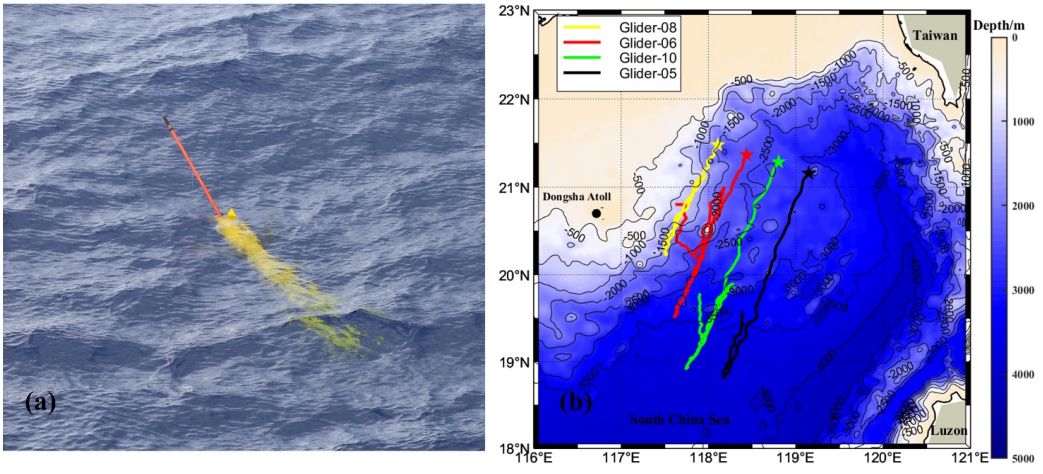

Figure 1(a) A Petrel-II glider at the surface for communication. (b) The trajectories of 4 gliders deployed in the active region of internal solitary waves, whose starting positions are presented by pentagrams.

During this survey, four gliders yielded 647 profiles and traveled 1907.7km cumulatively (Table 1). In most profiles, gliders dived into 900~1000m deep, except in a few profiles they did shallow dives to 600m, considering the steep terrain near the Dongsha Atoll. For the purpose of obtaining high-resolution data, each glider was set to run with a vertical velocity of 0.1~0.15m/s by adjusting the net buoyancy and pitch angle, and thus, it took 2~5 hours for the gliders to perform a sawtooth profile with 2~5 km horizontal distance. Each glider is equipped with a Seabird

https://doi.org/10.5194/os-2021-29
Preprint. Discussion started: 23 April 2021

GPCTD, sampling at 1Hz to record the thermohaline fluctuation with a high resolution when the ISWs pass. Therefore, the high sampling frequency and low gliding velocity enable the maximum thermohaline resolution to be 0.15m in vertical and 2.5km in spatial scales.

Table 1 Summary of the cooperative observation by several gliders in August, 2017

No.	Deployment	recovery	profiles	distance (km)
Glider-05	08.04	08.18	146	397.7
Glider-06	08.04	08.28	195	627.6
Glider-08	08.05	08.21	121	310.5
Glider-10	08.04	08.29	185	571.9
Total	/	/	647	1907.7

3 Estimation of vertical water velocities

The glider's sawtooth movement in longitudinal plane can be described by the kinematic model (Leonard and Graver, 2001). Affected by the vertical variations of seawater physical properties and pressure hull deformation, the net driven force of glider is gradually varied with depth, which causes the glider to perform non-uniform speed movement during the phase of diving or climbing. However, the acceleration of glider is far below its velocity in these phases, and acceleration values have a negligible influence on the velocity on a small-time scale. Hence, except buoyancy changes at the beginning and turning point of profiles at the maximum depth, the stable underwater motion can be deemed as quasi-steady flight, and the theoretical or still-water vertical velocities (w_g) of glider can be estimated by the kinematic equations, which has been derived in the Ma et al.(2018). The actual vertical velocitiy (w_p) calculated from pressure sensor is the sum of the vertical water velocity (w_c) and theoretical velocity (w_g) (Merckelbach et al., 2010). Consequently, w_c can be yielded as

$$w_c = w_p - w_g \tag{1}$$

The core of estimating w_c based on the glider lies in the kinematic model. Most of parameters (such as mass, pitch angle, etc.) in the model are measured through the sensors or tools, but part of parameters, including hydrodynamics coefficients (C_{D0}, C_D, C_{L0}, C_L), coefficient of compressibility (γ), thermal expansion coefficient (ε), and glider volume at atmospheric pressure (V_g) are indirectly estimated by the empirical formulas or computer simulations. In addition, gliders work underwater for several days or even months. Therefore, the parameter variations in the model arising from uncertainties have a remarkable effect on the vertical water velocities. For example, biofouling can increase the drag force of glider. The model coefficients can be identified and calibrated by minimizing cost function (Merckelbach et al., 2010; Frajka-Williams et al., 2011; Merckelbach et al., 2019).

Considering the complex calculation and coupled nonlinear coefficients in the model, influence of parameter variations on the vertical water velocities remains to be determined. A local sensitivity analysis is adopted to explore the effect of parameter uncertainty on the results, and most obvious factors are optimized by applying a standard nonlinear search method (Merckelbach et al., 2010).

Gliders work in the time-varying marine environment, so the data acquired in the stable upward motion, where the roll is zero and the pitch is constant, are input into the glider model, and the sensitivity of each indirectly estimated parameter which could influence the theoretical vertical velocity is quantificationally presented with single factor

https://doi.org/10.5194/os-2021-29
Preprint. Discussion started: 23 April 2021

Ocean Science
Discussions
Open Access
EGU

variance analysis. A different boundary condition of each variable is set in numeric computation. During sensitivity analysis of structural parameters, the glider volume V_g fluctuates $\pm$10mL around the original value, whereas coefficient of compressibility (γ) or thermal expansion coefficient (ε) varies ±10% around the original value. The effects of those parameters on mean theoretical vertical velocity are calculated separately, and the results are shown in Fig. 2(a).

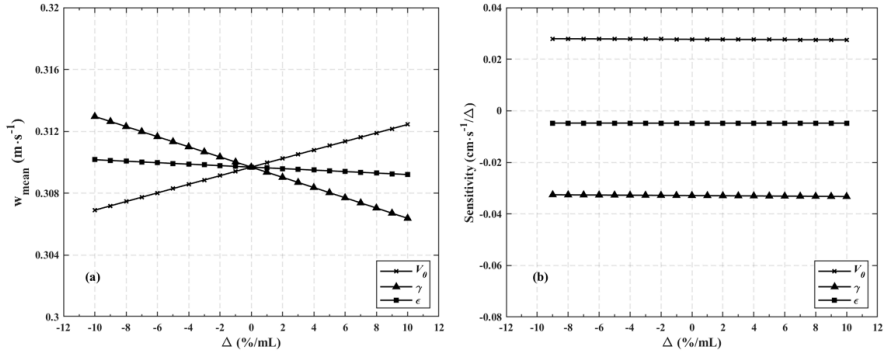

Figure 2 The sensitivity analysis of structural parameters (V_g, γ ε). (a) The influence of parameter variation on the mean vertical velocity of model. (b) The sensitivity of parameters in the mean vertical velocity of model.

The results of Fig. 2(a) reveal that the mean theoretical vertical velocity w_g increases approximately linearly with glider volume V_g. As shown in Eq. (5) (Ma et al., 2018), the driven force in the climbing phase augments with V_g, and that results in an increased vertical velocity when the other parameters are constant. By contrast, the mean w_g reduces gradually as the increasing coefficient of compressibility (γ) or thermal expansion coefficient (ε), which is caused by the reduction of buoyancy force. The sensitivity of those structural parameters to mean w_g is referred in Fig. 2(b), and the sensitivity of V_g, γ and ε to the mean vertical velocity is 0.0274~0.079 cm•s^{-1}/*ml*, -0.032~-0.033cm •s^{-1}/Δ and -0.004 cm•s^{-1}/Δ (Δ denotes a variation rate of 1%), respectively. The sensitivity of ε is lower than others. Thereby, the compressibility coefficient (γ) and glider volume (V_g) have a greater influence on the theoretical vertical velocities.

Similarly, the sensitivity of hydrodynamic coefficients (C_{D0}, C_D, C_{L0}, C_L) is analyzed. As is clear in Fig. 3(a), the mean w_g reduces gradually as the increase of C_{D0} or C_L, while the mean w_g changes little along with the increasing C_D or C_{L0}. The sensitivity of mean w_g to those hydrodynamic coefficients is given in Fig. 3(b). The sensitivity of C_{D0} and C_L is -0.11~-0.07 cm•s^{-1}/Δ and -0.068~-0.047 cm•s^{-1}/Δ, respectively, while the sensitivity of C_D or C_{L0} is close to zero.

https://doi.org/10.5194/os-2021-29
Preprint. Discussion started: 23 April 2021

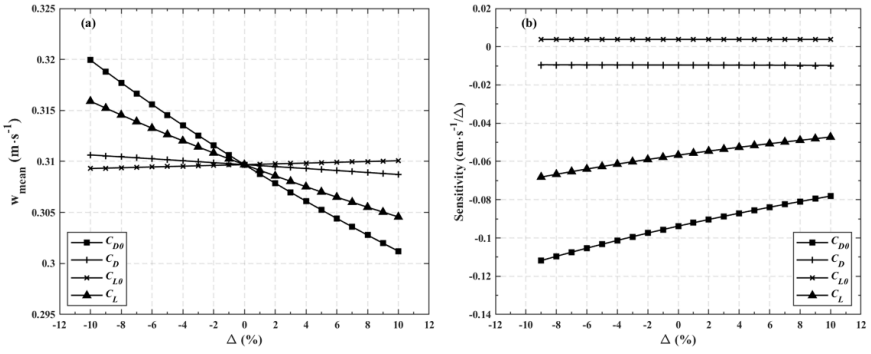

Figure 3 The sensitivity analysis of hydrodynamic coefficients (C_{D0}, C_D, C_{L0} and C_L). (a)The influence of coefficient variations on the mean vertical velocity of model. (b) The sensitivity of coefficients to the mean vertical velocity of model.

According to the sensitivity analysis results, structural parameters (V_g, γ) and hydrodynamic coefficients (C_{D0}, C_L) own a high sensitivity to the theoretical vertical velocities (w_g), while others cause an influence on w_g with the order of $\boldsymbol{O}(10^{-3})$, which can be ignored. Therefore, those high-sensitivity factors are ameliorated by minimizing the cost function F, thus to reduce the error of estimated vertical water velocities (Merckelbach et al., 2010).

Given the variable running depth and unstable motion in the phase of pumping oil, the data obtained at depths shallower than 600 m are utilized for the minimization process. Those optimized parameters as a function of dive number are shown in Fig. 4.

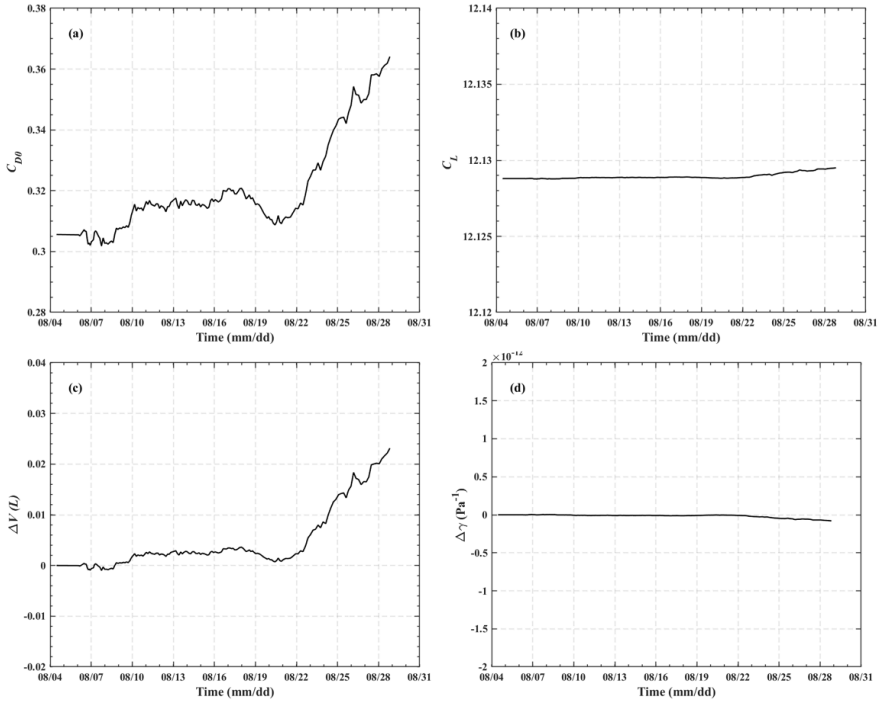

Figure 4 Optimized parameters versus time. (a) drag coefficient. (b) lift coefficient. (c) glider volume. (d) compressibility coefficient.

https://doi.org/10.5194/os-2021-29
Preprint. Discussion started: 23 April 2021

The optimization results show that the drag coefficient C_{D0} increases with working time. The biofouling by barnacles and film-like sludge is the main reason that causes drag increase. Those attachments are clearly visible on the recovered glider (Fig. 5). However, the lift coefficient C_{L0} has no significant difference relative to C_{D0}. The buoyancy change generates driving force for glider's sawtooth motion. When the glider dives into the target depth, the hydraulic oil are pumped into the external bladder from the inner tank inside the pressure hull. Under the influence of repeated cold-heat cycles, the air bubbles dissolved in the oil are separated, and occupy a small proportion of the inner tank volume, which gradually increase with the number of profiles. Petrel-II glider adjusts its net buoyancy according to the detected volume change of the inner tank. The air bubbles lead to the fluctuation of glider volume V_g, and still exist in the inner tank when we maintain the glider after recovery. Those air bubbles may influence the compressibility γ of glider.

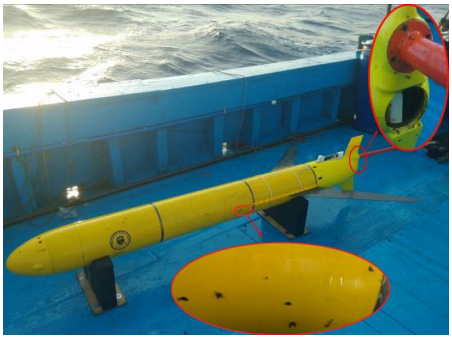

Figure 5 The biofouling on the glider hull. The surface of glider is attached by the barnacles and film-like sludge.

The structural parameters can be validated through the depth-keeping experiment. The glider's buoyancy should be equivalent to its gravity to keep the glider in the constant depth. Hence, this motion can be realized by setting appropriate buoyancy. The depth-keeping experiment and simulations with original and corrected structural parameters are shown in Fig. 6. The experiment lasted for about half an hour, and the glider held depth at 848±1m. Substituting the original and corrected parameters V_g and γ separately into the buoyancy model yields the depth simulations, and the error of depth decreases from 24m to 12m when corrected parameters are adopted.

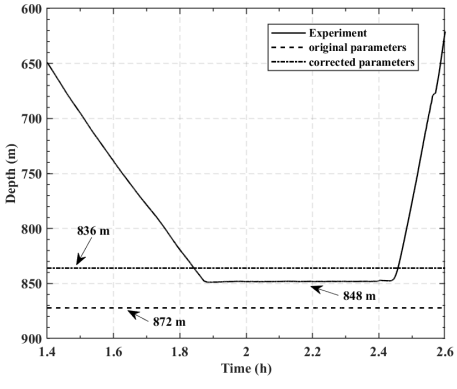

Figure 6 Comparison between simulation and depth-keeping experiment. The error is reduced by half with the adoption of corrected parameters.

https://doi.org/10.5194/os-2021-29
Preprint. Discussion started: 23 April 2021

Ocean Science
Discussions
Open Access
EGU

188 The glider vertical velocity w_p relative to water velocity is obtained by the time rate of change of pressure
189 measured by the CTD, but those signals contain noises, or even glitches. Due to the excellent time-frequency
190 characteristic, the wavelet transform is applied to restrain those noises. Based on the vertical velocity estimation
191 method and optimized parameters, the water and glider vertical velocities are achieved, as shown in Fig. 7.

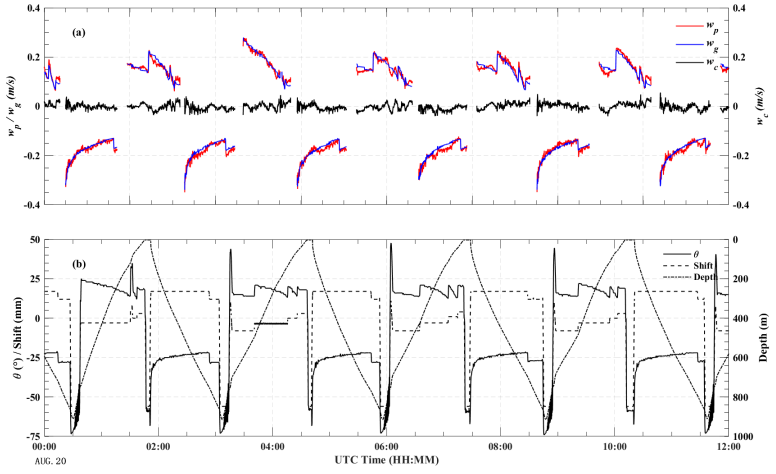

192
193 Figure 7 Vertical velocity, pitch, shift, depth versus time. Given the unsteady motion during the eccentric battery pack shifting or rotating,
194 and variable buoyancy engine working, the velocities in those moment are excluded.

195 The tendency of theoretical velocity (w_g) is coincident with that of vertical velocity (w_p) in Fig. 7. The error of
196 the estimation of vertical water velocity inferred from glider data is mainly due to the mixed sampled noise and the
197 inaccuracy of parameters in the model. It is difficult to compare the estimated results with the vertical velocities
198 measured independently in the field. A robust approach to estimate the vertical water velocities is proposed in the
199 reference (Merckelbach et al., 2010). The mean vertical water velocities for 3-day periods are 2.22±0.41mm/s after
200 parameter optimization, and the fluctuation of mean values in the adjacent bins of 50m is below 0.1mm/s, showing
201 that values share well continuity in the vertical direction. Over the same time periods, the offset of vertical water
202 velocity between dives and climbs is -2.9±1mm/s. Therefore, the inaccuracy of vertical water velocity estimated from
203 glider data is nearly 4mm/s.

204 ## 4 Identifying internal solitary waves

205 Four gliders conducted the observation cooperatively in the mission, moved southwestward and then traveled
206 backward. The vertical water velocities are calculated with the method described in Section 3. We analyze the vertical
207 water velocities within the common depth from 50m to 500m during the steady gliding motion. Therefore, the spatial
208 distribution of the standard deviation (*std*) of w_c during each dive in this region from 4 August to 16 August is mapped
209 out as shown in Fig. 8. The pink chain-dotted lines denote the observing time at intervals of 1 day.

https://doi.org/10.5194/os-2021-29
Preprint. Discussion started: 23 April 2021

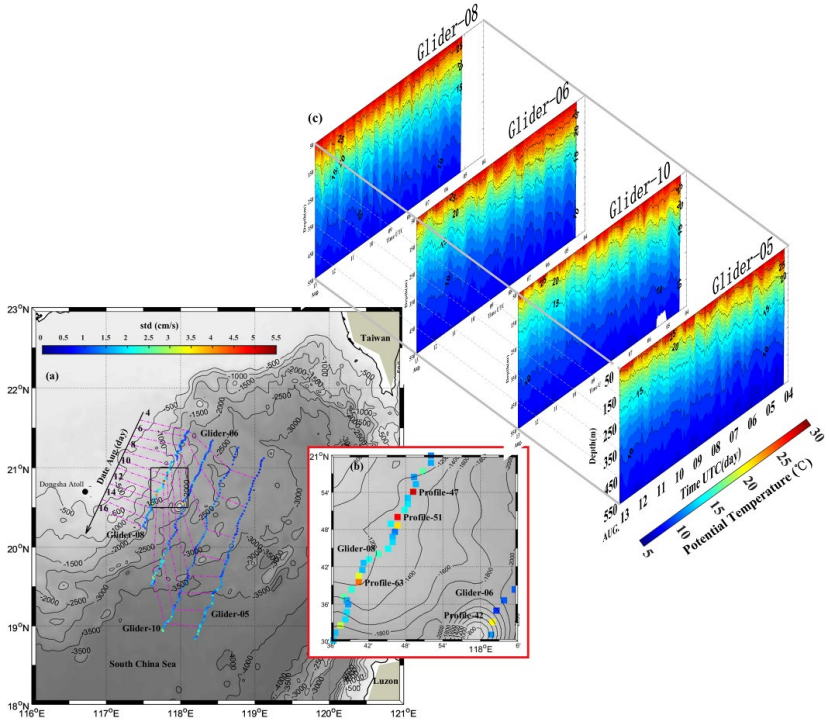

Figure 8 (a) Spatial distribution of the standard deviation (std) of w_c, (b) the dramatic *std* in the observation region of Glider-08, and (c) potential temperature obtained by glider-based GPCTD between 4 August and 12 August (50m~500m). Color shadings and contour lines are isothermals at 1°C intervals. Isothermal surfaces of 10, 15, 20, and 25°C are labeled.

The *std* of inferred vertical water velocities during each glider dive exhibits a significant variation in the coverage area of observation, and can be denoted the turbulent mixing or the internal wave strength (Beaird et al., 2012; Todd, 2017; Evans et al., 2018). This variation indirectly reflects that the activity of vertical water increases gradually at the same latitude along the east-west direction, and such distribution coincides with fluctuation of isotherms in the 4 temperature transections measured by glider-based CTD. This phenomenon may be due to the combination of the nonlinear effects and topographic effects when the waves are propagating westward (Simmons et al., 2011).

The average *std* of all inferred vertical velocity profiles is 1.5±0.5 cm/s within that depth range. Glider-08 encounters violent vertical flow when passing the rough topography in the survey, which may be caused by the passage of ISWs on the east side of Dongsha Atoll, shown in Fig. 8(b). The standard deviations of vertical velocities present a dramatic rise up to 5.06cm/s (20°54.08′N, 117°49.23′E), 4.83cm/s (20°50.02′N, 117°46.67′E), and 4.22cm/s (20°39.48′N, 117°40.42′E), respectively, and these values are considerably larger than the average.

Waves with various structures, namely depression wave and elevation wave, can cause disparate fluctuation of thermohaline structures. The passing depression wave forces isotherms to move sharply down, while the passing elevation wave induces an opposite displacement (Fu et al., 2012). In addition to thermohaline fluctuations, another notable phenomenon induced by ISWs is the sharp horizontal water velocity, and those ISWs in the northeastern SCS propagate westward at a speed in the order of 0.72 to 1.8 m/s (Liu et al., 2004). With the aid of hydrodynamic force

https://doi.org/10.5194/os-2021-29
Preprint. Discussion started: 23 April 2021

Ocean Science
Discussions
Open Access
EGU

generated by wings, the horizontal velocity of glider is typically about 0.2~0.4m/s. The horizontal speed gap between glider and ISW can affect the way of encountering, so generally the ISW propagates past the glider. In other words, if an ISW passes the present position of glider, the glider cannot capture this wave again whichever direction the glider travels along, even the glider travels along the direction of the wave propagation.

Generally, the magnitude of vertical water velocities induced by ISWs is larger than that of the background velocities before arrival of ISWs. The occurrence of ISWs can be reflected by the vertical water velocities estimated by the glider (Rudnick et al., 2013). This, together with characteristic of ISWs, can be used to further analyze those extraordinary profiles in Fig. 8(b). The time series of vertical water velocities and depth of three continuous profiles (No.46/47/48) performed by Glider 08 are shown in Fig. 9.

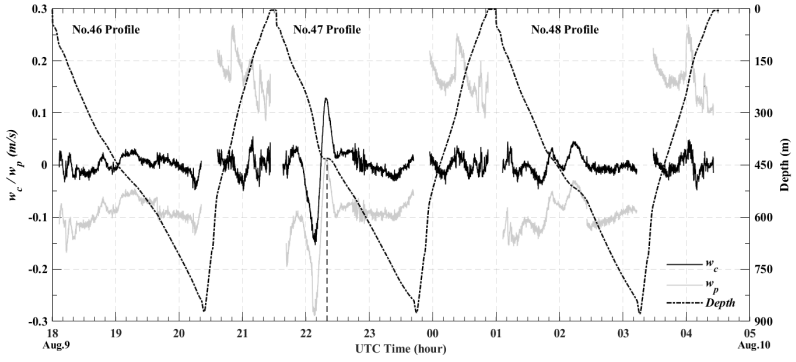

Figure 9 The vertical velocities derived from Glider08 data and depth as a function of time

As obvious from Fig. 9, the vertical water velocity derived from Profile-47 experiences a dramatic fluctuation at the depth 150-450m in the diving phase. As the depth increases, the vertical currents present large downward velocities, which then convert into upward velocities in less than 40 min, and the peak magnitudes of upwelling and downwelling are about 0.13 m/s and 0.14 m/s, respectively. The strong upwelling forces the glider to change its predefined movement direction from downward to upward at 22:20 UTC. After that, the vertical currents present a relatively gradual change, and in the adjacent profiles, no significant perturbations appear in the vertical dimension. Taking the chronological change of vertical waver velocities into consideration, this rapid phenomenon occurring during the diving process of Profile-47 is consistent with the passage of the abrupt ISW. Only a complete peak-to-trough vertical velocity oscillation over such a period of time suggests that the wave is likely a single-wave ISW.

The glider can synchronously acquire thermohaline structure with the payload CTD, and the thermal stratification is shown in Fig. 10. The passage of ISWs captured by Profile-47 induced sunken displacements of isothermals, and this phenomenon coincides with characteristics of a depression ISW.

https://doi.org/10.5194/os-2021-29
Preprint. Discussion started: 23 April 2021

Ocean Science
Discussions
Open Access
EGU

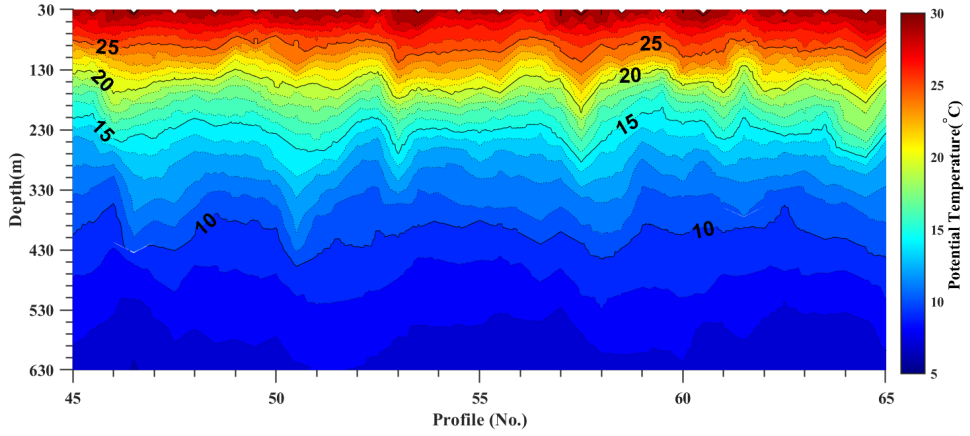

Figure 10 Thermal structural distribution obtained by Profiles 45~65 (Glider-08)

Another interesting phenomenon occurs in profiles 61~65. As is clear in Fig. 10, it seems that a small depression wave arrived in profile-61, making the thermocline sunk to nearly 300m depth. Then the thermocline quickly recovered in the following profiles 62~65 suggesting that the wave influencing profile-61 had already passed. After that, the isothermals at water depths from 100m to 400m fluctuate dramatically again in profile-65, which may be impacted by another depression wave.

The vertical water velocities derived from those profiles of the glider are taken for further analysis. In clear contrast to relatively stable thermohaline structure in profiles-62~65, the vertical water velocities of those profiles exhibit consecutively periodic oscillations as illustrated in Fig. 11. The vertical velocities of the wave completing a cycle of peak- trough- peak oscillate in the form of a simple sinusoidal independent of time (Todd, 2017). Given that the horizontal velocity of glider is far smaller than the propagation speed of ISW, the glider cannot cross the same ISW again. Those consecutively sinusoidal oscillations of vertical water velocities inferred from Profile-63 are likely influenced by a multiple-wave packet with a train of rank-ordered ISWs.

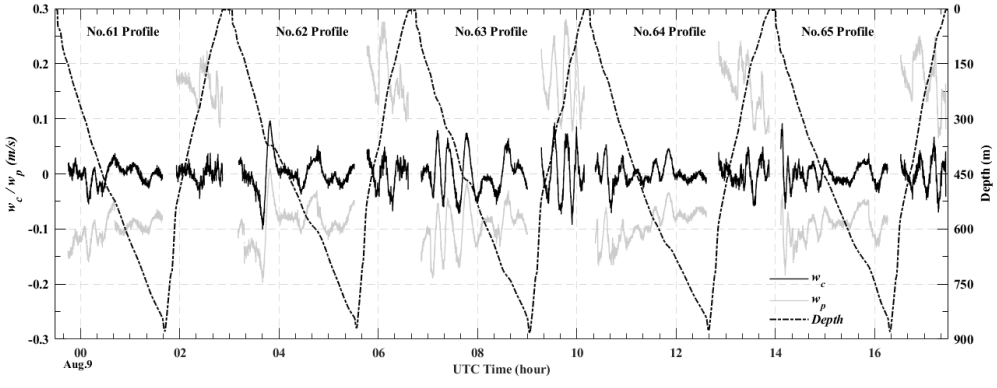

Figure 11 Vertical velocity, depth versus time of Profiles 61~65 (Glider-08)

The ISWs cause the change of roughness on the sea surface, and alter the sun-glint reflection. These characteristics are presented with the bright or dark strips in the satellite images, which is often used to catalog the

https://doi.org/10.5194/os-2021-29
Preprint. Discussion started: 23 April 2021

Ocean Science
Discussions
Open Access
EGU

occurrence of ISWs (Zhao et al., 2004). One true-color MODIS (Moderate Resolution Imaging Spectroradiometer) satellite image (Fig. 12) with 250m-resolution taken on 12 August 2017 at 3:15 UTC presents a snapshot of the active internal waves in the South China Sea. The image displayed in a partially enlarged frame clearly shows the existence of two types of waves, a single-wave ISW (left arrow pointing) and a multiple-wave packet (right arrow pointing). Coincidentally, the Glider-08 conducting the No.62 profile (Fig. 11) is located at the western edge of the multiple-wave packet at the same time. Since the waves propagate westward, there is a high possibility that glider-08 captures the multiple-wave packet in the continuous profiles, and the probability is verified by the oscillation of vertical water velocities inferred from glider.

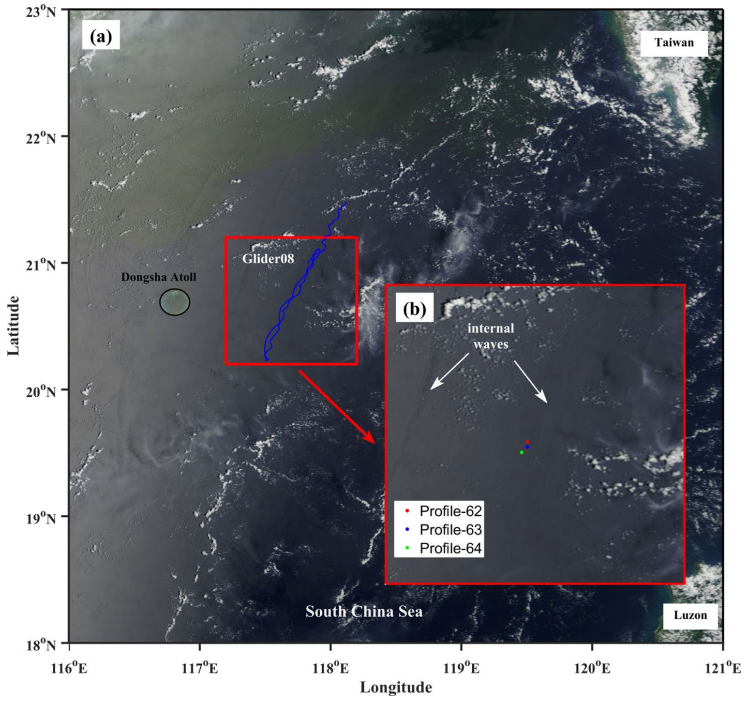

Figure 12 A MODIS true-color image of ISWs (resolution: 250m) in the South China Sea acquired at 03:10 UTC, Aug.12, 2017. The blue line in (a) is the Glider 08's trajectory. The red solid box is enlarged in (b), and the red, blue and green points denote the valid GPS position of No.62, 63 and 64 profiles, respectively.

The thermohaline structure obtained by glider-based CTD reflects less features of ISWs than the vertical water velocities inferred from glider data. This is due to the movement characteristics of glider. The sawtooth motion of glider makes it unable to suspend at an appointed position for a long time, and thus the glider cannot carry out the measurement of the vertical seawater properties at multiple depths synchronously, which is adopt by the sensor chains in the mooring. Considering the significant speed differences between glider and ISW, it is so hard to determine whether the thermohaline perturbation observed by glider-based CTD is induced by a single-wave or multiple-wave packet, and even whether there exist waves within the spurious stable thermohaline stratification inferred from glider-based CTD data.

The vertical water velocities deduced by the glider provide a robust evidence that ISWs have passed by the

https://doi.org/10.5194/os-2021-29
Preprint. Discussion started: 23 April 2021

glider's current position. The opposite vertical velocities are generated on the leading and trailing edges of wave along its propagation direction (Ramp et al., 2004). Ideally, the oscillation of vertical water velocities presents a sinusoidal form when the glider passes successively through the leading and trailing edges of a wave, and this phenomenon occurs continuously if the glider flies through a multiple-wave ISW packet. Hence, it is more intuitionistic and accurate to determine the existence and type of the ISW by analyzing the feature of vertical water velocities inferred from glider, and this method is tested to be practicable. Further, in combination with the convex or concave isotherms/isohalines obtained by glider-based CTD, the characteristic (depression or elevation) of wave can be determined.

5. Summary and discussion

We applied several underwater gliders to observe internal waves in the South China Sea. Without extra current sensors, the vertical water velocity is derived through the combination of the quasi-steady flight model and sea-trial data of glider. The accuracy of parameters in the model directly determines the credibility of the inferred velocity. Therefore, the local sensitivity analysis method is applied to discuss the parameters in the model, which cannot be measured exactly by the sensors or tools. The results indicate that structural parameters (V_g, γ) and hydrodynamic coefficients (C_{D0}, C_L) are the main factors affecting the accuracy of the inferred vertical water velocity. Those predominant parameters are calibrated by nonlinear optimization algorithm. Furthermore, the hover experiment validates the effect of the optimized structural parameters, and the error of depth range is reduced by half of the amount. With the same error estimation method of Slocum gliders (Merckelbach et al., 2010), the accuracy of the inferred vertical water velocity is nearly 4mm/s.

The observation with 4 gliders is conducted in the SCS. The *std* of the inferred vertical water velocity during each dive characterizes the strength of vertical water activity, and exhibits a gradual increase in the same latitude along the east-west direction in the coverage area of observation. This phenomenon is coincident with the fluctuation of isotherms.

A few profiles, where the *std* of vertical water velocity is larger than the average *std,* are further analyzed. Since those gliders are deployed in the region between Dongsha Atoll and Luzon Strait, where ISWs occur with high-frequency in July and August (Zheng et al., 2007), the dramatic vertical water mass flow may be attributed to the propagation of ISWs. The glider traveling along with the sawtooth motion cannot maintain a fixed position like moorings to obtain complete thermohaline stratification at different depths before and after ISWs arrival. Therefore, the common identifying and classifying method of ISWs using the temperature structure measured by glider CTD may miss the key feature of ISWs.

Given vertical flow induced by the passage of ISWs, the vertical water velocity inferred from glider, together with the thermohaline perturbation, is utilized to identify the ISWs. The vertical velocities of the wave in a complete cycle peak- trough- peak experience an approximate sinusoidal oscillation. The horizontal speed gap between the glider flying and ISW propagation determines that the glider cannot travel across the same ISW repeatedly. Therefore, analysis of the vertical water velocity oscillation in the velocity profile with remarkable *std* and adjacent profiles helps to determine whether the encountered wave is a single- or multiple-wave ISW packet. Glider-08 captures different kinds of ISWs in the sea-trial, and the method is proven to be feasible and effective by comparison with a

https://doi.org/10.5194/os-2021-29
Preprint. Discussion started: 23 April 2021

MODIS image. Furthermore, according to the sunken isothermals, those captured waves are classified as depression waves.

This paper investigates the activity of internal waves in the eastern area of Dongsha Atoll and proposes a method of identifying the type of ISWs, which is applicable to glider observation. Although gliders may enable us to obtain high-resolution observation data, there are comparable challenges to estimate the key parameters of ISWs, such as propagation direction and the phase velocities. Direct velocity measurements using current meters or current profilers on gliders might provide a solution to this problem. Future cooperative surveys with a fleet of gliders can be performed to understand the propagation and evolution of ISWs.

*Data availability. T*he MODIS image is available at https://earthdata.nasa.gov/earth-observation-data. Data from field experiments is available on request from wei.ma@tju.edu.cn or corresponding author.

Author contributions. Wei Ma carried out the research and initiated the paper. All the authors collected, processed and analyzed the observations and contributed to revisions and comments on the paper

Competing interests. The *authors* declare that they have no conflict of interest.

Acknowledgements. This work is supported by the National Natural Science Foundation of China (Grant Nos.52005365) and National Key R&D Program of China (Grant Nos. 2016YFC0301100).

References

Alford, M. H., Lien, R., Simmons, H., Klymak, J., Ramp, S., Yang, Y. J., Tang, D., and Chang, M.: Speed and evolution of nonlinear internal waves transiting the South China Sea, *J. Phys. Oceanogr.*, 40, 1338-1355, https://doi.org/10.1175/2010JPO4388.1, 2010.

Beaird, N., Fer, I., Rhines, P., Eriksen, C.: Dissipation of Turbulent Kinetic Energy Inferred from Seagliders: An Application to the Eastern Nordic Seas Overflows, *J. Phys. Oceanogr.*, 42, 2268-2282, https://doi.org/10.1175/JPO-D-12-094.1, 2012.

Boettger, D., Robertson, R., and Rainville, L.: Characterizing the semidiurnal internal tide off Tasmania using glider data, *J. Geophys. Res.-Oceans*, 120, 3730-3746, https://doi.org/10.1002/2015JC010711, 2015.

Cai, S. Q., Xie, J. S., and He, J. L.: An overview of internal solitary waves in the South China Sea, *Surv. Geophys*.,33, 927-943, https://doi.org/10.1007/s10712-012-9176-0, 2012.

Cai, S. Q., Xie, J. H., and Xu, J. X., Wang, D. X., Chen, Z. W., Deng, X. D., and Long, X. M.: Monthly variation of some parameters about internal solitary waves in the South China Sea, *Deep-Sea Res. Pt. I*, 84: 73-85, https://doi.org/10.1016/j.dsr.2013.10.008, 2014.

Evans, D.G., Lucas, N.S., Hemsley, V., Frajka-Williams, E., Naveira Garabato, A.C., Martin, A., Painter, S.C., Inall, M.E., Palmer, M.R.: Annual cycle of turbulent dissipation estimated from seagliders, *Geophys. Res. Lett*., 45, 10560-10569, https://doi.org/10.1029/2018GL079966, 2018.

Frajka-Williams, E., Eriksen, C.C., Rhines, P.B., Harcourt, R.R.: Determining vertical water velocities from seaglider,

https://doi.org/10.5194/os-2021-29
Preprint. Discussion started: 23 April 2021

367 *J. Atmos. Ocean. Tech.,* 28, 1641-1656, https://doi.org/10.1175/2011JTECHO830.1, 2011.
368 Farmer, D. M., Alford, M. H., Lien, R. C., Yang, Y. J., Chang, M. H., and Li, Q.: From Luzon Strait to Dongsha
369 Plateau: stages in the life of an internal wave, *Oceanography*, 24, 64-77,
370 https://doi.org/10.5670/oceanog.2011.95, 2011.
371 Fu, K., Wang, Y. H., Laurent, L. S., Simmons, H., and Wang, D. P.: Shoaling of large-amplitude nonlinear internal
372 waves at Dongsha Atoll in the northern South China Sea, *Cont. Shelf. Res.*, 37,1-7,
373 https://doi.org/10.1016/j.csr.2012.01.010, 2012.
374 Hall, R., Berx, B., and Inall, M.: Observing internal tides in high-risk regions using co-located ocean gliders and
375 moored ADCPs, *Oceanography*, 30(SI), 51-52, https://doi.org/10.5670/oceanog.2017.220, 2017.
376 Hall, R. A., Berx, B., and Damerell, G. M.: Internal tide energy flux over a ridge measured by a co-located ocean
377 glider and moored acoustic doppler current profiler, *Ocean Sci.*, 15, 1439-1453, https://doi.org/10.5194/os-15-
378 1439-2019, 2019.
379 Huang, W. G., Johannessen, J., Alpers, W., Yang, J., and Gan, X.: Spatial and temporal variations of internal wave
380 sea surface signatures in the northern South China Sea studied by spaceborne SAR imagery, In: Proceedings of
381 the 2nd SeaSAR Symposium. Frascati, Italy, 1-6. 2008.
382 Huang, X. D., Chen, Z. H., Zhao, W., Zhang, Z. W., Zhou, C., Yang, Q. X., and Tian, J. W., An extreme internal
383 solitary wave event observed in the northern South China Sea, *Sci. Rep.*, 6, https://doi.org/10.1038/srep30041,
384 2016.
385 Jackson, C.: Internal wave detection using the moderate resolution imaging spectroradiometer (MODIS). *J. Geophys.*
386 *Res.-Oceans*, 112, https://doi.org/10.1029/2007JC004220, 2007.
387 Johnston, T. M. S., and Rudnick, D. L.: Trapped diurnal internal tides, propagating semidiurnal internal tides, and
388 mixing estimates in the California Current System from sustained glider observations, *Deep-Sea Res. Pt. II*,
389 112(SI), 61-78, https://doi.org/10.1016/j.dsr2.2014.03.009, 2015.
390 Johnston, T. M. S., Rudnick, D. L., and Kelly, S. M.: Standing internal tides in the Tasman Sea observed by gliders,
391 *J. Phys. Oceanogr.*, 45, 2715-2737, https://doi.org/10.1175/JPO-D-15-0038.1, 2015.
392 Leonard, N. E., and Graver, J. G.: Model-based feedback control of autonomous underwater gliders, *IEEE J. Oceanic*
393 *Eng.*, 26, 633-645, https://doi.org/10.1109/48.972106, 2001.
394 Liang, J. J., Li, X. M., Sha, J., Jia, T., and Ren, Y. Z.: The lifecycle of nonlinear internal waves in the northwestern
395 South China Sea, *J. Phys. Oceanogr.*, 49, 2133-2145, https://doi.org/10.1175/JPO-D-18-0231.1, 2019.
396 Liu, A. K., Ramp, S. R., Zhao, Y., and Tang, T. Y.: A case study of internal solitary wave propagation during ASIAEX
397 2001, *IEEE J. Oceanic. Eng.*, 29, 1144-1156, https://doi.org/10.1109/JOE.2004.841392, 2004.
398 Ma, W., Wang, Y. H., Yang, S. Q., Wang, S. X., and Xue, Z.: Observation of internal solitary waves using an
399 underwater glider in the northern South China Sea, *J. Coastal. Res.*, 34, 1188-1195,
400 https://doi.org/10.2112/JCOASTRES-D-17-00193.1, 2018.
401 Merckelbach, L., Smeed, D., and Griffiths, G.: Vertical water velocities from underwater gliders, *J. Atmos. Ocean.*
402 *Tech.*, 27, 547-563, https://doi.org/10.1175/2009JTECHO710.1, 2010.
403 Merckelbach, L., Berger, A., Krahmann, G., Dengler, M., Carpenter, J.R.: A dynamic flight model for Slocum gliders
404 and implications for turbulence microstructure measurements, *J. Atmos. Ocean. Tech.*, 36, 281-296,

https://doi.org/10.5194/os-2021-29
Preprint. Discussion started: 23 April 2021

https://doi.org/10.1175/JTECH-D-18-0168.1, 2019.

Ramp, S. R., Tang, T. Y., Duda, T. F., Lynch, J. F., Liu, A. K., Chiu, C. S., Bahr, F. L., Kim, H. R., and Yang, Y. J.: Internal solitons in the northeastern South China Sea, Part I: Sources and deep water propagation. *IEEE J. Oceanic. Eng.*, 29, 1157-1181, https://doi.org/10.1109/JOE.2004.840839, 2004.

Ramp, S. R., Yang, Y. J., and Bahr, F. L.: Characterizing the nonlinear internal wave climate in the northeastern South China Sea, *Nonlinear. Proc. Geoph.*, 17, 481-498, https://doi.org/10.5194/npg-17-481-2010, 2010.

Rudnick, D. L., Johnston, T. M. S., and Sherman, J. T.: High-frequency internal waves near the Luzon Strait observed by underwater gliders, *J. Geophys. Res.-Oceans*, 118, 774-784, https://doi.org/10.1002/jgrc.20083, 2013.

Rudnick, D. L.: Ocean research enabled by underwater gliders, *Annu. Rev. Mar. Sci.*, 8, 519-541, https://doi.org/10.1146/annurev-marine-122414-033913, 2016.

Shroyer, E. L., Moum, J. N., and Nash, J. D.: Vertical heat flux and lateral mass transport in nonlinear internal waves, *Geophys. Res. Lett.*, 37, https://doi.org/ 10.1029/2010GL042715, 2010.

Simmons, H., Chang, M. H., Chang, Y. T., Chao, S. Y., Fringer, O., Jackson, C. R., and KO, D. S.: Modeling and prediction of internal waves in the South China Sea, *Oceanography*, 24(SI): 88-99, https://doi.org/ 10.5670/oceanog.2011.97, 2011.

Testor, P., de Young, B., Rudnick, D. L., Glenn, S., Hayes, D., Lee, C. M., Pattiaratchi, C., Hill, K., Heslop, E., Turpin, V., Alenius, P., Barrera, C., Barth, J. A., Beaird, N., Becu, G., Bosse, A., Bourrin, F., Brearley, J. A., Chao, Y., Chen, S., Chiggiato, J., Coppola, L., Crout, R., Cummings, J., Curry, B., Curry, R., Davis, R., Desai, K., DiMarco, S., Edwards, C., Fielding, S., Fer, I., Frajka-Williams, E., Gildor, H., Goni, G., Gutierrez, D., Haugan, P., Hebert, D., Heiderich, J., Henson, S., Heywood, K., Hogan, P., Houpert, L., Huh, S., Inall, ME., Ishii, M., Ito, S., Itoh, S., Jan, S., Kaiser, J., Karstensen, J., Kirkpatrick, B., Klymak, J., Kohut, J., Krahmann, G., Krug, M., McClatchie, S., Marin, F., Mauri, E., Mehra, A., Meredith, M. P., Meunier, T., Miles, T., Morell, J. M., Mortier, L., Nicholson, S., O'Callaghan, J,. O'Conchubhair, D., Oke, P., Pallas-Sanz, E., Palmer, M., Park, J., Perivoliotis, L., Poulain, P. M., Perry, R., Queste, B., Rainville, L., Rehm, E., Roughan, M., Rome, N., Ross, T., Ruiz, S., Saba, G., Schaeffer, A., Schonau, M., Schroeder, K., Shimizu, Y., Sloyan, B. M., Smeed, D., Snowden, D., Song, Y. M., Swart, S., Tenreiro, M., Thompson, A., Tintore, J., Todd, R. E., Toro, C., Venables, H., Wagawa, T., Waterman, S., Watlington, R. A., Wilson, D.: OceanGliders: A component of the integrated GOOS, *Front. Mar. Sci.*, 6, https://doi.org/10.3389/fmars.2019.00422, 2019.

Todd, R. E.: High-frequency internal waves and thick bottom mixed layers observed by gliders in the gulf stream, *Geophys. Res. Lett.*, 40, 6316-6325, https://doi.org/ 10.1002/2017GL072580, 2017.

Whitt, C., Pearlman, J., Polagye, B., Caimi, F., Muller-Karger, F., Copping, A., Spence, H., Madhusudhana, S., Kirkwood, W., Grosjean, L., Fiaz, B. M., Singh, S., Singh, S., Manalang, D., Sen Gupta, A., Maguer, A., Buck, J. J. H., Marouchos, A., Atmanand, M. A.,. Venkatesan, R., Narayanaswamy, V., Testor, P., Douglas, E., de Halleux, S., and Khalsa, S. J.,: Future vision for autonomous ocean observations, *Front. Mar. Sci.*, 7, https://doi.org/10.3389/fmars.2020.00697, 2020.

Zhao, Z. X., Klemas, V., Zheng, Q. A., and Yan, X. H.: Remote sensing evidence for baroclinic tide origin of internal solitary waves in the northeastern South China Sea, *Geophys. Res. Lett.*, 31, https://doi.org/10.1029/2003GL019077, 2004.

https://doi.org/10.5194/os-2021-29
Preprint. Discussion started: 23 April 2021

443 Zheng, Q. A., Susanto, R. D., Ho, C. R., Song, Y. T., and Xu, Q.: Statistical and dynamical analyses of generation
444 mechanisms of solitary internal waves in the northern South China Sea, *J. Geophys. Res.-Oceans*, 112,
445 https://doi.org/10.1029/2006JC003551, 2007.